Extracting photon periodic orbits from spontaneous emission spectra in laterally confined vertically emitted cavities

Yung-Fu Chen,* Yan-Ting Yu, Yu-Jen Huang, Po-Yi Chiang, Kuan-Wei Su, and Kai-Feng Huang

Department of Electrophysics, National Chiao Tung University, Hsinchu, Taiwan
**Corresponding author: yfchen@cc.nctu.edu.tw*

Received March 22, 2010; revised June 21, 2010; accepted July 16, 2010;
posted July 21, 2010 (Doc. ID 125825); published August 10, 2010

We report our observation of the signature of photon periodic orbits in the spontaneous emission spectra of large-aperture vertical-cavity surface-emitting lasers (VCSELs). The high-resolution measurement clearly demonstrates that over a thousand cavity modes with a narrow linewidth can be perfectly exhibited in the spontaneous emission spectrum just below the lasing threshold. The Fourier-transformed spectrum is analyzed to confirm that the spontaneous emission spectra of large-aperture VCSELs can be exploited to analogously investigate the energy spectra of the 2D quantum billiards. © 2010 Optical Society of America

OCIS codes: 140.3410, 140.5960, 260.5740.

Optical microcavities have great potential for applications in miniature lasers, biological sensors, optical telecommunications, and basic research on modern physics [1–4]. Recently, large-aperture oxide-confined vertical-cavity surface-emitting lasers (VCSELs), serving as an analogous quantum billiard, have been employed to explore the quantum wave functions in mesoscopic systems [5–7]. An interesting phenomenon has been observed in that the electromagnetic field distributions of the lasing modes are mostly localized on the periodic ray trajectories, signifying the particle-wave duality [7]. Nowadays, periodic orbits are ubiquitously recognized as the most prominent feature in a wide range of systems, including particle accelerators [8], atomic spectra [9], and astronomy [10]. To the best of our knowledge, all studies to date related to photon periodic orbits have been restricted lasing spectra [2,5,6,11], and none has explored the role of photon periodic orbits from spontaneous emission spectra. As proposed by Purcell [12], the spontaneous emission rate of a radiating system can be significantly modified by using a cavity to tailor the coupling of an emitter with the vacuum field. This question naturally arises: would it be possible that photon periodic orbits play an important role in the spontaneous emission of an emitter in the large-aperture microcavity?

In this Letter we fabricate a large-aperture square-shape oxide-confined VCSEL to explore the spontaneous emission spectra in very high resolution. Experimental results clearly reveal that the coupling effects between the optical modes and the spontaneous emission increase with the increase of the injection current. We observed that several thousand cavity modes can be almost perfectly displayed in the spontaneous emission spectra. The Fourier transform of the spontaneous emission spectrum just below the lasing threshold reveals a recurrence spectrum in which each photon periodic orbit appears a peak in a plot of intensity versus length. This finding casts light on the new application of large-aperture VCSELs in studying the energy spectra of 2D quantum billiards with spontaneous emission spectra.

In this investigation, the VCSEL device, grown with metal–organic chemical vapor deposition, consists of a multiple quantum-well active region and doped semiconductor distributed Bragg reflector (DBR) mirrors to form the vertical cavity. The active region comprises three $Al_{0.07}Ga_{0.93}As$-$Al_{0.36}Ga_{0.64}As$ quantum wells with well and barrier thickness of 70 and 100 Å, respectively. The spacers at both sides of a quantum well were added to form a $1-\lambda$ cavity. For exploring the optical mode spectrum by electroluminescence spectroscopy, a large detuning between the quantum-well ground-state exciton and the fundamental cavity mode was designed. The detuning magnitude was approximately $\Delta\omega/2\pi = 2.7$ THz. The periods for the top and bottom DBR mirrors are 23 and 29, respectively. A high Al composition $Al_{0.97}Ga_{0.03}As$ layer is placed at the first positive-DBR mirror, which is oxidized for current and optical confinement. The device processing was carried out as follows. The wafers were wet oxidized at 425 °C, and the oxidation time is controlled to fabricate a 40 μm oxide square aperture in a 110 μm mesa structure.

Schematics of the laser device structure and the experimental setup are shown in Fig. 1. The VCSEL device was placed in a temperature-controlled system with a stability of 0.1 °C near room temperature. A current source with a precision of 0.01 mA was utilized to drive the VCSEL device. The emitted pattern was reimaged onto a CCD camera with a very-large-NA microscope objective lens (Mitutoyo, NA = 0.9) mounted on a translation stage. The spectral information of the radiation output

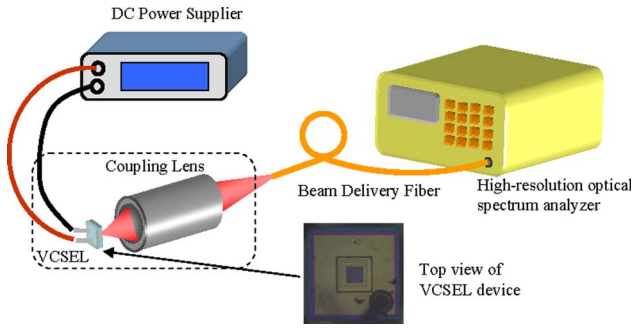

Fig. 1. (Color online) Schematics of the laser device structure and the experimental setup.

 © 2010 Optical Society of America

was measured by a high-resolution optical spectrum analyzer (Advantest Q8347). The present spectrum analyzer employs a Michelson interferometer with a Fourier spectrum system to reach a resolution of 0.002 nm; consequently, the cavity-mode spectral information can be resolved to a large extent.

Figures 2(a)–2(e) depict the emission spectra measured for several injection currents. Below the lasing threshold of 26 mA, the scale of the modulation depth in the emission spectra was clearly seen to deepen with an increase of the injection current, as shown in Figs. 2(a)–2(e). The presence of sharp emission peaks arises from the high-Q optical confinement and each peak at the injection current of 25 mA [Fig. 2(d)] is clearly resolved with less background. These peaks not only correspond to optical resonance modes but also signify the fact that transition probabilities are enhanced for emission wavelengths near the optical modes. As shown in the inset of Fig. 2(d), the linewidth of each isolated optical mode can be down to narrower than 0.01 nm. Because the linewidth of the quantum-well emitter is 10^3 – 10^4 wider than the average mode spacing of the cavity mode, there are several thousand cavity modes to be almost perfectly exhibited in the spontaneous emission spectra. More specifically, all the observed modes are the transverse modes of the cavity [13]. The change of cavity finesse with current indicates that the observed spectra should be referred to as the amplified spontaneous emission. When the injection current amounts to 26 mA, a few optical modes reach the lasing threshold and start to dominate the emission intensity, as seen in Fig. 2(e).

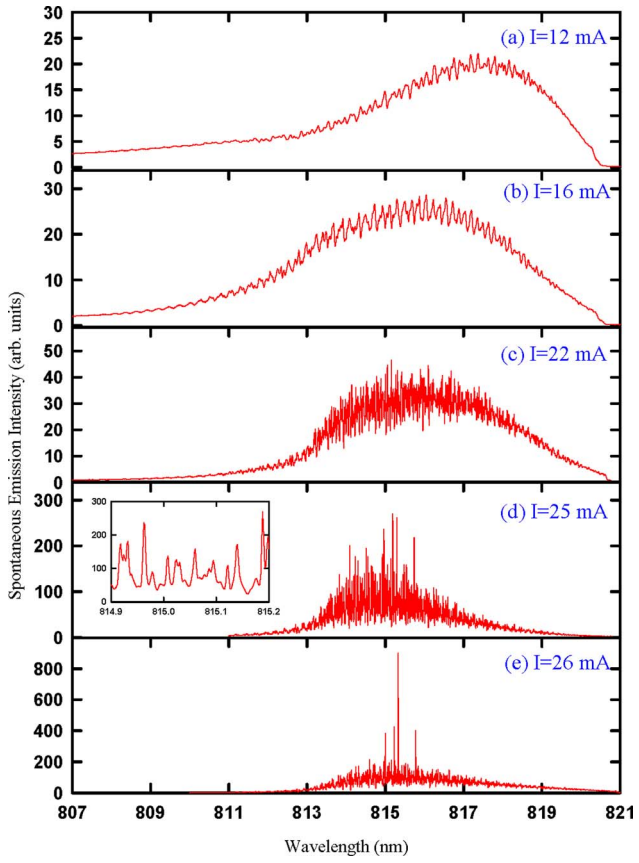

Fig. 2. (Color online) Emission spectra measured for several injection currents: (a)–(d) below lasing threshold and (e) just above lasing threshold.

It has been confirmed that the character of classical periodic orbits can be extracted from observed quantum spectra with a Fourier transform [14–16]. Analogously, the Fourier transform of the amplified spontaneous emission spectra should exhibit resonances corresponding to photon periodic orbits in VCSEL cavities. Because the longitudinal wavenumber in the VCSEL device is unique and given by $k_z = 2\pi/\lambda_o$, the experimental amplified spontaneous emission spectrum can be interpreted as the equivalent 2D density of state $\rho_{\mathrm{SE}}(K) = \sum_n \delta(K - K_n)$, where K is the variable for the transverse wavenumber, $K_n = \sqrt{k_n^2 - k_z^2}$, $k_n = 2\pi/\lambda_n$, and λ_n are the observed cavity modes. As a consequence, the Fourier transform of the amplified spontaneous emission spectrum with K as the variable is given by $\tilde{\rho}_{\mathrm{SE}}(L) = \int \mathrm{d}K \rho_{\mathrm{SE}}(K)\, e^{iKL} = \sum_n e^{iK_nL}$, where the sum is over all observed wavenumbers and L is the conjugate variable of the wavenumber. To be precise, $\tilde{\rho}_{\mathrm{SE}}(L)$ represents the autocorrelation function of the amplified spontaneous emission spectrum and each peak showing up in $|\tilde{\rho}_{\mathrm{SE}}(L)|$ is associated with the length of a resonant ray orbit. Note that the value of λ_o can be determined by the longest emission wavelength in the experimental spectrum. As shown in Fig. 2(a), the value of λ_o is approximately 820.8 nm. Numerical analysis reveals that the extracted resonant lengths were found to be almost unchanged for the value of λ_o varying within 820.8 ± 0.1 nm.

Figures 3(a)–3(e) depict the Fourier-transformed spectra $|\tilde{\rho}_{\mathrm{SE}}(L)|$, corresponding to the spontaneous emission spectra shown in Figs. 2(a)–2(e), respectively. It can be also seen that below the lasing threshold, the higher the current is injected, the more resonance peaks appear in $|\tilde{\rho}_{\mathrm{SE}}(L)|$. This result indicates that the coupling strength between the optical modes and the spontaneous emission spectra increase with increasing the injection current. The origin of the resonance peaks in $|\tilde{\rho}_{\mathrm{SE}}(L)|$ can be confirmed to be associated with the photon periodic orbits in the transverse plane. In a square lateral confinement, the formation of periodic orbits for photons undergoing specular reflection at each side wall is subject to the conditions of $k_x/k_y = p/q$, where p and q are two integers and k_x and k_y are the x component and y component of the transverse wavenumber, respectively. The path length of the periodic orbit $(p,\ q)$ is then given by $L(p,q) = 2a\sqrt{p^2 + q^2}$, where a is the length of the square boundary. Note that if p and q have common factors, such an orbit categorically corresponds to a recurrence of a simpler one in which the photon undergoes two or more periods. As seen in Figs. 3(a)–3(d), the resonance peaks in $|\tilde{\rho}_{\mathrm{SE}}(L)|$ are in good agreement with the results of the geometric orbits, which manifest the importance of the photon periodic orbits in spontaneous emission spectra. More intriguingly, the discernible orbits $(p,\ q)$ become more and more complex as the injection current increases. On the other hand, Fig. 3(e) illustrates that just above the lasing threshold, the stimulated emission significantly affects the interplay between the optical modes and the spontaneous emission, causing the elimination of the resonance peaks in $|\tilde{\rho}_{\mathrm{SE}}(L)|$. Recently,

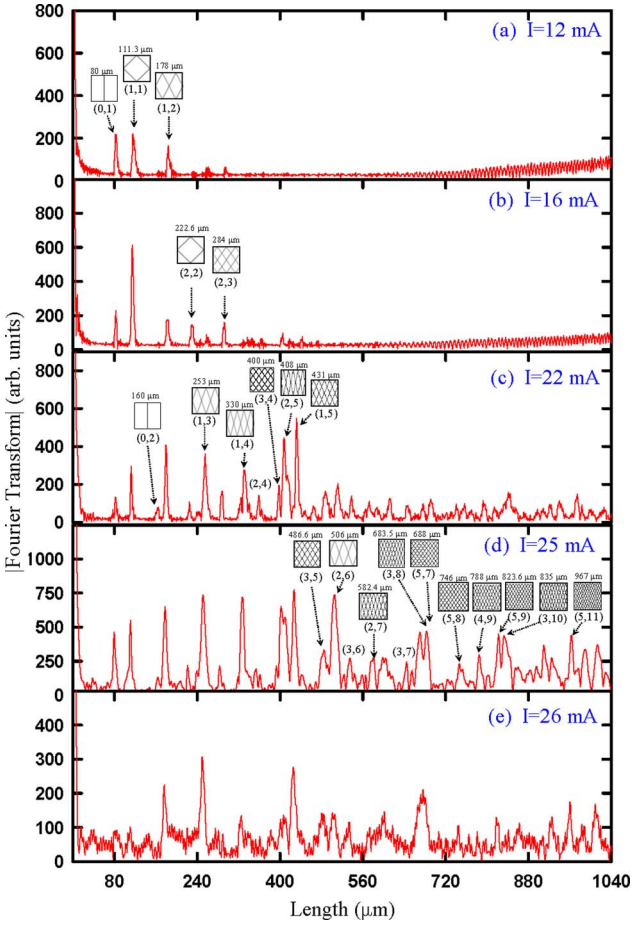

Fig. 3. (Color online) Fourier-transformed spectra $|\tilde{\rho}_{SE}(L)|$, corresponding to the spontaneous emission spectra shown in Figs. 2(a)–2(e), respectively.

Du *et al.* [17] theoretically found that the concept of periodic-orbit theory can be extended from electron to photon in analyzing the spontaneous emission rate of an atom near a dielectric interference. It is the first time, to our knowledge, to discover the significance of photon periodic orbits in the feature of the spontaneous emission spectra of large-aperture VCSELs, as found in the atomic absorption spectra [18]. More importantly, it is worth mentioning that there was no obvious difference in the spectra from sample to sample for devices growth in the same batch.

In conclusion, we have performed very-high-resolution measurement to demonstrate the signature of photon periodic orbits in the spontaneous emission spectra of large-aperture VCSELs. The coupling effects between the optical modes and the spontaneous emission are found to increase with an increase in the injection current. Just below the lasing threshold, we have observed that more than a thousand cavity modes with a narrow linewidth are precisely displayed in the spontaneous emission spectra. The resonant peaks that appeared in the Fourier-transformed spectrum are verified to excellently coincide with the theoretical ones obtained from the 2D square quantum-billiard model. Based on all the agreement, large-aperture VCSELs can be confirmed to function as "photonic billiards," and their spontaneous emission spectra can be employed to analogously investigate the energy spectra of quantum billiards.

This work is supported by the National Science Council of Taiwan (NSCT) (contract NSC-97-2112-M-009-016-MY3).

References

1. C. Gmachl, F. Capasso, E. E. Narimanov, J. U. Nöckel, A. D. Stone, J. Faist, D. L. Sivco, and A. Y. Cho, Science **280**, 1556 (1998).
2. M. Lebental, N. Djellali, C. Arnaud, J. S. Lauret, J. Zyss, R. Dubertrand, C. Schmit, and E. Bogomolny, Phys. Rev. A **76**, 023830 (2007).
3. T. Tanaka, M. Hentschel, T. Fukushima, and T. Harayama, Phys. Rev. Lett. **98**, 033902 (2007).
4. J. Wiersig and M. Hentschel, Phys. Rev. Lett. **100**, 033901 (2008).
5. K. F. Huang, Y. F. Chen, H. C. Lai, and Y. P. Lan, Phys. Rev. Lett. **89**, 224102 (2002).
6. T. Gensty, K. Becker, I. Fischer, W. Elsässer, C. Degen, P. Debernardi, and G. P. Bava, Phys. Rev. Lett. **94**, 233901 (2005).
7. Y. F. Chen, K. F. Huang, and Y. P. Lan, Phys. Rev. E **66**, 066210 (2002).
8. D. Robin, C. Steier, J. Laskar, and L. Nadolski, Phys. Rev. Lett. **85**, 558 (2000).
9. D. M. Wang and J. B. Delos, Phys. Rev. A **63**, 043409 (2001).
10. V. Szebehely, *Theory of Orbits* (Academic, 1967).
11. M. Schulz-Ruhtenberg, I. V. Babushkin, N. A. Loiko, T. Ackemann, and K. F. Huang, Appl. Phys. B **81**, 945 (2005).
12. E. M. Purcell, Phys. Rev. **69**, 37 (1946).
13. D. Wintgen, Phys. Rev. Lett. **58**, 1589 (1987).
14. M. Schulz-Ruhtenberg, I. V. Babushkin, N. A. Loiko, K. F. Huang, and T. Ackemann, Phys. Rev. A **81**, 023819 (2010).
15. I. V. Zozoulenko, A. S. Sachrajda, P. Zawadzki, K. F. Berggren, Y. Feng, and Z. Wasilewski, Semicond. Sci. Technol. **13**, A7 (1998).
16. K. F. Berggren, K. N. Pichugin, A. F. Sadreev, and A. Starikov, JETP Lett. **70**, 403 (1999).
17. M. L. Du, F. H. Wang, Y. P. Jin, Y. S. Zhou, X. H. Wang, and B. Y. Gu, Phys. Rev. A **71**, 065401 (2005).
18. M. L. Du and J. B. Delos, Phys. Rev. Lett. **58**, 1731 (1987).